Influence of flow conditions in porous asphalts on pollution and cleaning

Dipl.-Ing. Matthias A. Haselbauer
Prof. Dr.-Ing. Michael Manhart

Fachgebiet Hydromechanik, Technische Universität München, Germany

ABSTRACT

Porous asphalt pavements are used to reduce traffic noise and the danger of aqua-planing. After a few years, the benefit of these kinds of asphalts will deteriorate because of dust and particle pollution of the asphalt. The particles enter the pores of the asphalt and close them. The flow of water through the porous structure of the asphalt is hindered, which increases the danger of aquaplaning. Moreover, traffic noise is reflected by these particles and cannot be dissipated inside the porous structure. The asphalt loses its acoustic performance and has to be cleaned.
In order to be able to develop a satisfactory cleaning device, it is mandatory to understand the pollution mechanisms. In a concept of numeric simulations and experimental tests the fundamental questions of flow inside the porous asphalt pavements are investigated. In a first step the hydromechanic performance of the asphalts was determined. In laboratory tests the flow resistance of different porous asphalts was determined. Numerical simulations inside the porous structure helped to understand the inhomogeneous flow distribution and thereby the pollution mechanisms of porous asphalts.
To explain the self-cleaning effects of these asphalts by traffic, CFD simulations were set up to investigate the pressure and velocity fields inside the asphalt when a car passes at 80 km/h. On the basis of these results and the examination of traditional cleaning devices like high-velocity water jets, new approaches of cleaning these asphalts were developed. Better cleaning devices extend the life of porous asphalt layers and increase acoustic and flow performance of older asphalts.

1. Introduction

Open-pore asphalt (OPA) pavements are often used to combine two fundamental benefits. On the one hand, the OPA reduces traffic noise. Acoustic waves can enter the pore structure of OPA where they are dissipated. On the other hand, water can penetrate the OPA. Thus, at rain events less spray in the air improves the sight for drivers and reduces the danger of aquaplaning. After a few years, the OPA-pavements loose their noise reducing performance due to dust pollution. Dust particles enter the pores of the asphalt and close them. Acoustic waves are reflected, which leads to a higher noise level. Moreover, the flow of water through the porous structure of the asphalt is hindered, which increases the danger of aquaplaning. To extend the useful life of use of these asphalts, the “Bundesanstalt für Straßenwesen” in Germany originated the joint project “Leiser Straßenverkehr 2”. Within this project, various partners work on a better understanding of physics in OPA and on a sustained noise reducing performance. Within the joint project, the Fachgebiet Hydromechnanik of the Technische Universität München is investigating the conditions of water and air flow at different boundary conditions. For this analysis, both laboratory experiments and numerical simulations are carried out, which are complementing one another. The aim of the project is the development of pollution avoiding techniques for OPA and the development of better cleaning procedures. Subsequently to the project, the theoretically found solution will undergo practical tests.

2. Fundamental Questions

Before investigations into the flow conditions in OPA can be done, the fundamental questions of the project have to be defined, answers to which have to be in the project.

Practical experience shows that untravelled asphalt pavements pollute faster than travelled ones. Because of this fact, it may be assumed that the traffic-induced flow conditions in the OPA are able to avoid dust pollution or are able to clean these lanes. The understanding of these flow conditions admits insights to the pollution and transport mechanisms of OPA. When these mechanisms are known, a modified cleaning device can be designed and tested.

The actual idea about the function of OPA is that dust particles penetrate into the OPA from the upper side of the asphalt layer due to rain or traffic. The slope of the road induces a horizontal flow inside the OPA towards the boundaries of the road. With this flow the dust particles are transported and eliminated from the asphalt matrix. To proof these mechanisms of OPA drainage, experimental tests were set up. Additionally, numerical simulations support these tests with geometrical parameter studies.

In studies of spacious flow conditions in OPA with numerical methods, the asphalt is regarded as homogenous material with certain material parameters. To obtain these parameters, the laboratory pass-through test of porous media after Darcy was set up. Six different asphalts were used to determine the flow resistance of different OPAs. For more information about the anisotropy of the flow resistance and the inhomogeneity of the flow in the OPA, detailed numerical simulations of the pass-through in the resolved pores were done. The results of these simulations are velocity and shear stress distributions in the pore space. These distributions allow conclusions about pollution or

cleaning mechanisms. Moreover, the influence of the pore geometry on the velocity distribution can be determined.

The results of these questions lead to a good comprehension of pollution mechanisms of OPA. With this knowledge, the efficiency of existing cleaning mechanisms will be examined. Finally, the question should be answered how a good cleaning mechanism must look like to enhance the durability of OPA.

3 CFD-Simulation of OPA

In the laboratory experiment of Darcy (Haselbauer [2]), OPA was regarded as homogeneous material. The asphalt samples were passed through in the vertical direction only. The obtained flow resistance is the mean value over the volume of the sample. The objective of the research project was to find explanations for the pollution mechanisms of OPA as well. Thus, in numerical investigations, the flow was modelled in the pore structure of the OPA to draw conclusions from the shear forces within the pores. These shear forces are very important for the particle transport mechanisms which are responsible for pollution and cleaning.

4.1 Meshing

In one part of the joint project “Leiser Straßenverkehr 2” the “Bundesanstalt für Materialforschung und –prüfung” (BAM) in Berlin employs the computer tomography method to analyse the pore structure of OPA. The distribution of pores and of dust pollution in OPA is investigated. Within these analyses three-dimensional geometric models of the asphalt samples were obtained.

To analyse the flow inside of OPA, we used in a first step two different OPA cuboids whose geometry was built by the BAM. The first sample was a cuboid with 9 x 9 x 30 mm, the second one was a cube with an edge length of 29 mm. For the calculation of the flow, the commercially available CFD-tool CFX of ANSYS, Inc., should be used. The exchange format for the geometry was the stereolithography (STL) file format. With this geometry format we tried to generate a mesh with ICEM-CFD of ANSYS, Inc. After various attempts of meshing and after support of the development department of ANSYS the pore structure of OPA was found to be too complicated to generate a good mesh with this commercial tool. Because we could not use CFX without a good mesh, we decided to use the code MGLET, which was developed at the Technische Universität München and which was available for the calculations.

4.2 MGLET

The program code MGLET solves the incompressible Navier-Stokes equations:

$$\frac{\partial u_i}{\partial x_i} = 0 \tag{4}$$

$$\frac{\partial u_i}{\partial t} + u_j \frac{\partial u_i}{\partial x_j} = -\frac{1}{\rho}\frac{\partial p}{\partial x_i} + \nu \frac{\partial^2 u_i}{\partial x_j^2} \tag{5}$$

The Navier-Stokes equations are integrated within the standard framework of Finite Volumes using staggered Cartesian grids. The spatial approximations are second order accurate and use centered interpolations and differentiations. Time integration is performed via a fractional step method using a Leapfrog scheme with time lagged diffusion for the momentum equation (5):

$$u^{n+1} = u^{n-1} + 2\delta t(D(u^{n-1}) + C(u^n) + G(p^{n+1})) \tag{6}$$

Where (u) is the velocity field, (D) are the diffusive terms, (C) the convective and (G) the pressure terms. The pressure p^{n+1} is obtained by the Poisson equation:

$$div[G(\delta p^{n+1})] = -\frac{1}{2\delta t} div(u^{n+1}) \tag{7}$$

where u^{n+1} is an intermediate velocity field and $\delta p^{n+1} = p^{n+1} - p^n$. The resulting system is solved by Stone's strongly implicit procedure (SIP). See e. g. Ferziger and Peric [1] for a discussion of these standard methods. The solid boundaries are taken into account by the Immersed Boundary method [3]. The principle of meshing with this method is shown in figure 1.

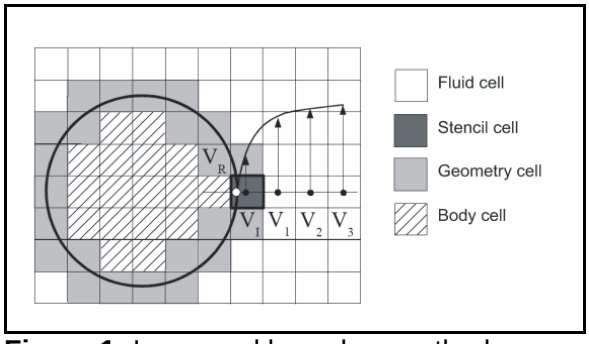

Figure 1: Immersed boundary method

With this meshing method, Cartesian meshes for the two cuboids were generated. After an analysis of the first simulation results, the smaller cuboid of 9 x 9 x 30 mm was found to be too small. As the effects of single pores were dominating, the results were not representative for spacious OPA. In the following simulations the larger cube of 29 x 29 x 29 mm only was used. For this geometry, a mesh of 256 x 256 x 256 = 16.6 x 10^6 cells was generated, which means a resolution of about 113 μm. In figure 2, the geometry of the test cube is plotted. The blue areas indicate regions of geometry, which can be filled with water, which corresponds to the pore volume. The grey regions are asphalt consisting of minerals and bitumen. The inhomogeneity of the pore distribution and of the pore radiuses is obvious.

To analyse the distribution of pores in the cube, cuts normal to the main axes were made at different locations. Such a cut comprises a 256 x 256 x 1 cell matrix. Across this matrix the ratio of fluid and asphalt cells was determined. The result is

illustrated in figure 3. The distribution of porosity along the x and y axis is more a less constant and ranges from 20 and 25 percent by volume. The maximum grain size of the asphalt was 8 mm. The changes in the porosity are influenced by single grains. The evaluation of the distribution along the z-axis shows an increase of porosity up to 45 percent by volume. This can be explained with the one-dimensional compaction process, as described earlier.

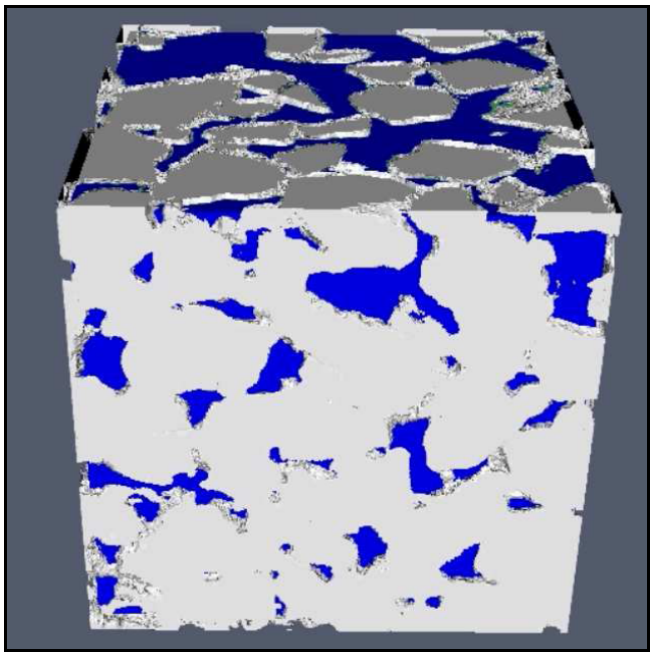

Figure 2: Geometry of the asphalt cube 29 x 29 x 29 mm

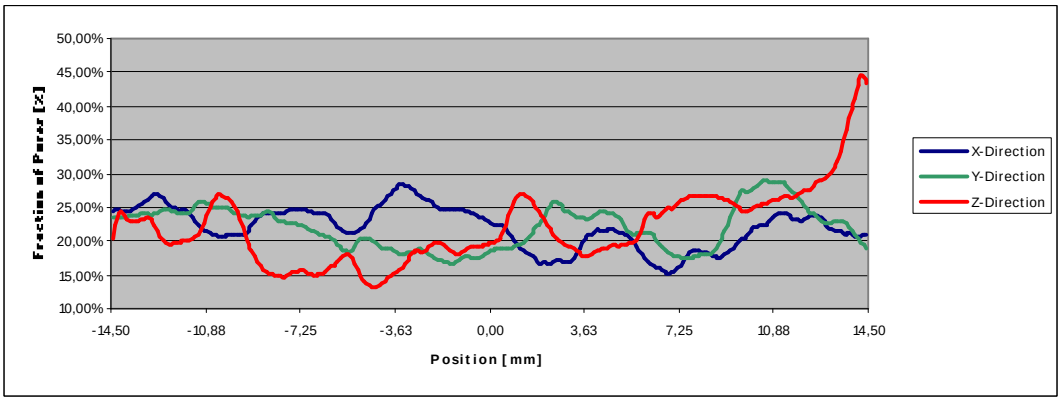

Figure 3: Distribution of porosity inside the asphalt cube

For the given geometry the vertical pass-through with water was simulated. As boundary condition (fig. 4), a static pressure difference of 10 Pa between the top and the bottom of the asphalt cube was chosen. The 10 Pa correspond to the hydrostatic pressure of 1 mm water column. At the horizontal boundaries, wall boundaries are used. This means, that no fluid can exit or enter the domain. At the wall, the tangential component of the velocity was set to zero, which is called a no-slip boundary condition. With the given boundary conditions, the fluid is accelerating asymptotically from zero to a resulting velocity field, at which the energy head loss is equal to the pressure difference.

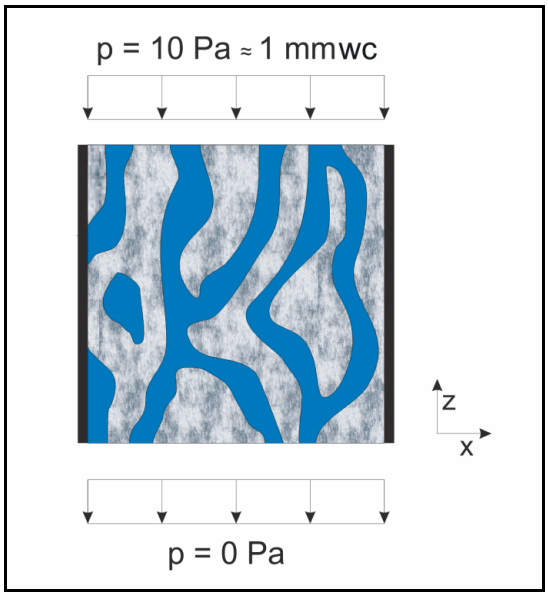

Figure 4: Boundary conditions of the simulations

The calculations were carried out at the super computing centre “Leibnitz Rechenzentrum” in Munich. With a parallelisation on 16 processors, each simulation took 48 hours at the SGI altix, a 64-bit Linux cluster. Thus, each simulation required more than 750 CPU-hours. The result of the vertical pass-through is plotted in figure 5. The streamlines of the flow are coloured with the velocity magnitude in millimetres per second.

Some pores of the test cube are connected quite well. This connection creates a short channel between the top and the bottom. In this channel, the resulting velocity magnitude is higher than 20 mm per second. The comparison of the mean flow rate of 0.348 mm/s and the highest velocities indicates a very inhomogeneous velocity distribution in the pore structure. The pores are all connected; there are no isolated holes in the structure. The mean porosity of the cube was 22.02 percent by volume. The values of the velocity evaluation are given in table 2. In 38.4 percent by volume of the pores, a significant velocity can be noticed. With this flow, pollution particles can be transported. But there can also be seen large areas with very small velocities within the structure. The pollution particles which enter these regions will rest there, and therefore these areas cannot be cleaned by water flow. It has to be noted, that these considerations are only valid for this special flow conditions at vertical pass-through. The

flow conditions can differ noticeable when the direction of the flow changes. Thus, regions which were not passed through by the flow in one case probably are passed at changed flow conditions in another case. Probably all regions are passed through in at least one special flow situation.

One possible approach for improving the drainage performance of the OPA could be to homogenise the pore geometry. If the value of 40.6% of pores where water with nearly zero velocity remains could be reduced significantly, pollution particles could be transported much easier. The success of cleaning devices would be considerably increased.

Finally, the simulations along different axis were compared. It can be seen (tab. 2) that the flow resistance along the z axis is the highest among the three values. This means that the flow resistance is inhomogeneous. Thus, when using the Darcy laws in numerical simulations, direction-dependent resistance parameters have to be considered. The given values in table 2 must be seen as single sample values. For a derivative of statistical values, a series of cubes have to be examined.

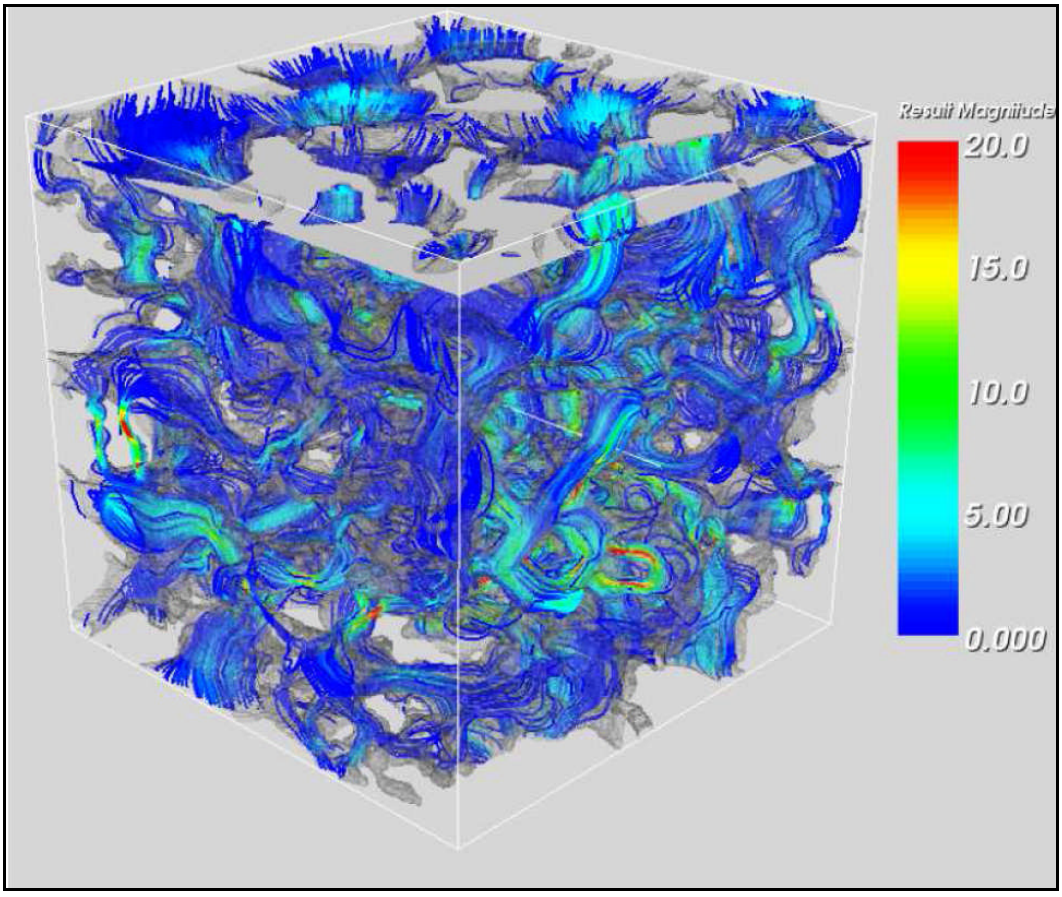

Figure 5: Streamlines in the asphalt cube

Table 1: Evaluation of the vertical pass through of the test cube 29 x 29 x 29 mm

Porosity of the test cube 29x29x29mm	22.02%
Fraction of pores with v > 1.0 mm/s	38.4%
Fraction of pores with 0.05 mm/s < v < 1.0 mm/s	21.0%
Fraction of pores with v < 0.05 mm/s	40.6%

Table 2: Evaluation of superficial fluid flow rates at different boundary conditions

Direction of the flow	X direction	Y direction	Z direction
Superficial fluid flow rate v	1.098 mm/s	0.762 mm/s	0.348 mm/s

After the fist simulations, we decided to improve the quality of the meshing algorithm. As can be seen in the principle figure 6, we smoothed the corners of the cut cells, which significantly increased the quality of the simulation results. Another advantage of the new algorithm is to maintain the wall normals as mesh information. In the project progress the wall shear stresses will be calculated, which will allow us to get informations about the forces onto the pollution particles.

With the new meshing method two other geometries of OPA were simulated. The geometry was built again by the BAM. The samples were of OPA 0/8, one was polluted and the other not. In figure 7, the geometry and the structure of the pore walls are displayed. The simulations were made once again with the code MGLET.

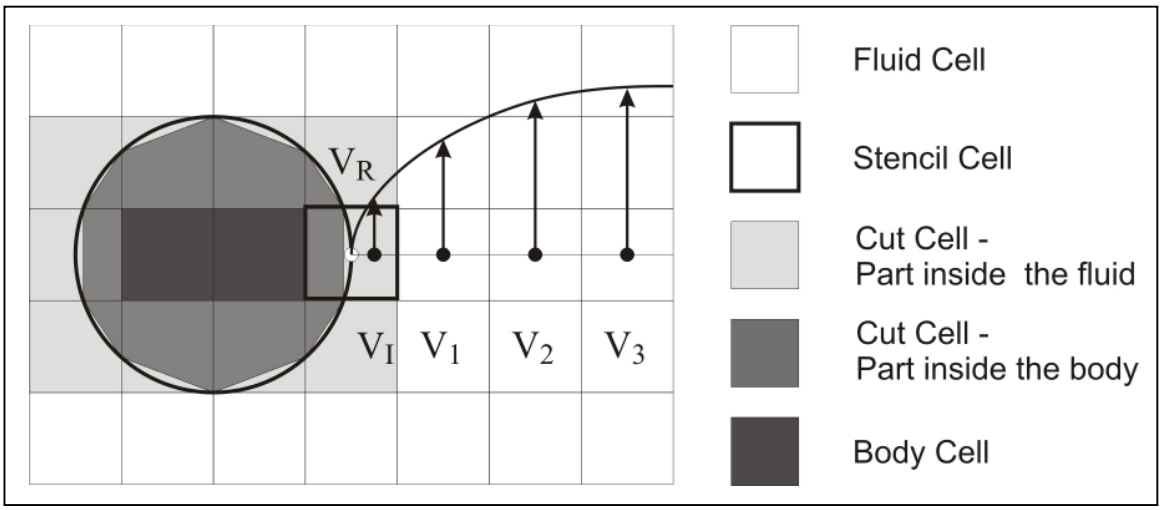

Figure 6: Improved immersed boundary method

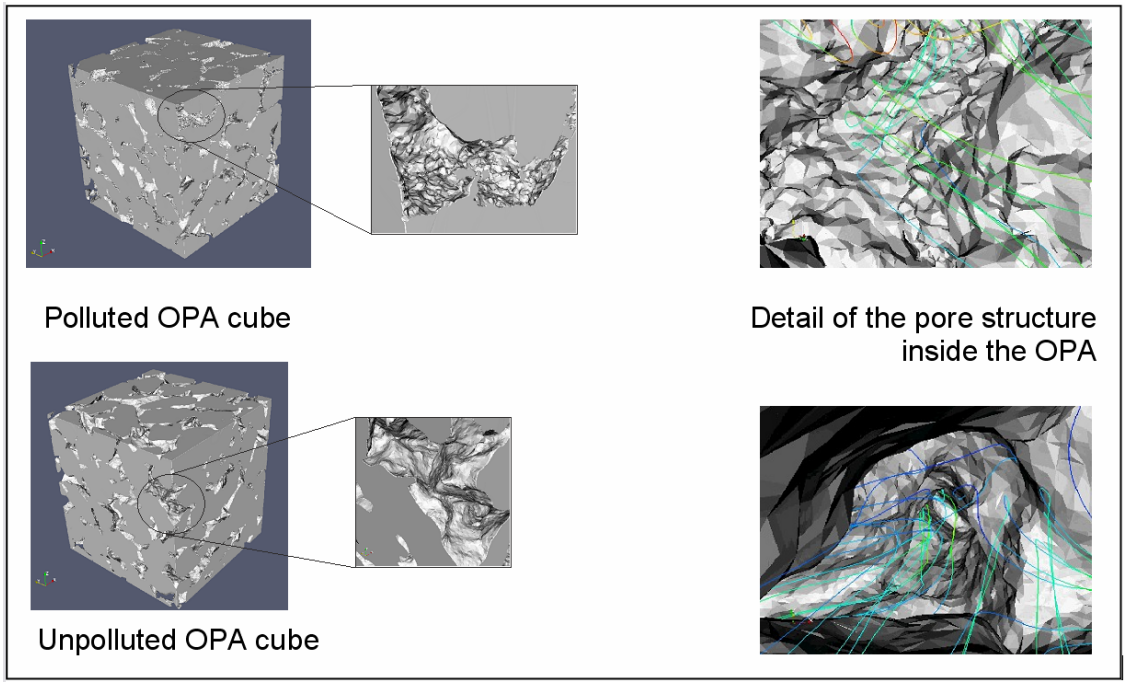

Figure 7: Geometry and the structure of the pore walls of the two OPA specimens

After the generation of the two meshes with 256 x 256 x 256 cells each the pore structure of the two specimens was initially examined, which differ quite enormously (tab. 3). The porosity of the unpolluted specimen is about 22 percent by volume and decreases to about 17 percent by volume in the polluted one. When examining the detailed pore structure, one can see that the pollution leads to a decrease of the pore diameters up to complete obstructing of single pore channels. This obstructing finally leads to a decrease of connected pore space. The complete pore space is significantly higher than the given 17 percent by volume. The difference consists of enclosed pore space were no fluid flow occurs.

In addition to the porosity, the volume fractions of the walls were calculated. The wall fractions, i.e. the percentages of the cells which are cut by walls are in both specimens almost equal with about 3.5 percent by volume. When adding the pore fraction to the consideration, an increase of the wall fractions can be observed. The reason for this observation is, on the one hand, a decrease of the pore diameters and thus a decrease of the ratio between perimeter and cross section. One the other hand, the inner walls of the pores get much rougher, as it can be seen in figure 7.

Table 3: Evaluation of the porosities and the volume fractions of the cells which are cut by walls of the two specimens

	Unpolluted cube	Polluted cube
Porosity of the sample cubes 30x30x30mm	22.03 %	17.19 %
Wall fraction of the specimen	3.859 %	3.43 %
Wall fraction of the pore space	17.51 %	19.94 %

In the simulations of the flow conditions the specimens were passed through along all three principle coordinate directions to proof the isotropy. The superficial fluid flow rates are almost equal comparing the three flow directions of the unpolluted specimen. With the pollution of the OPA, the flow resistance in the vertical direction increased four times, while the flow resistance in horizontal direction was only doubled. On the one hand, the observations led to a lower discharge, which decreased the capacities of particle transportation, and thus the drainability. Moreover, the pollution led to an over-proportional increase of the flow in vertical direction. The particles are transported significantly slower which increased and accelerated the pollution. Particles could enter the matrix but could not be transported inside the asphalt matrix.

Beside the superficial fluid flow rate, the velocity distributions inside the pore space were examined. The results were plotted in sum curves (figure 8). The distribution curves of the three flow directions of the unpolluted specimen are almost identical. The isotropy of the flow is demonstrated once again. Contrary to the unpolluted specimen, the sum curves of the polluted specimen differ significantly. The different horizontal and vertical distributions can be clearly seen. The vertical sum curve is shifted to the left side. The resulting lower velocities affect the particle transport mechanism negatively.

When comparing the sum curves of the polluted specimen and of the unpolluted specimen significant differences in the fraction of very low velocities can be observed. At the unpolluted OPA cube the fraction of cells with velocities lower than 0.1 mm/s is between 10 and 12 percent by volume. This fraction increases up to more than 27 percent by volume in the unpolluted specimen, which is more than twice this value.

The distributions of the fraction of velocities between 0.1 and 3mm/s are almost equal in all the specimens and directions, which can be seen in an almost equal gradient of the different curves. The fractions of high velocities become considerable smaller with the pollution.

Table 4: Evaluation of superficial fluid flow rates at different boundary conditions of the two specimens

Direction of the flow	X direction	Y direction	Z direction
Unpolluted specimen - Superficial fluid flow rate v	1.181 mm/s	1.081 mm/s	1.069 mm/s
Polluted specimen - Superficial fluid flow rate v	0.491 mm/s	0.434 mm/s	0.247 mm/s

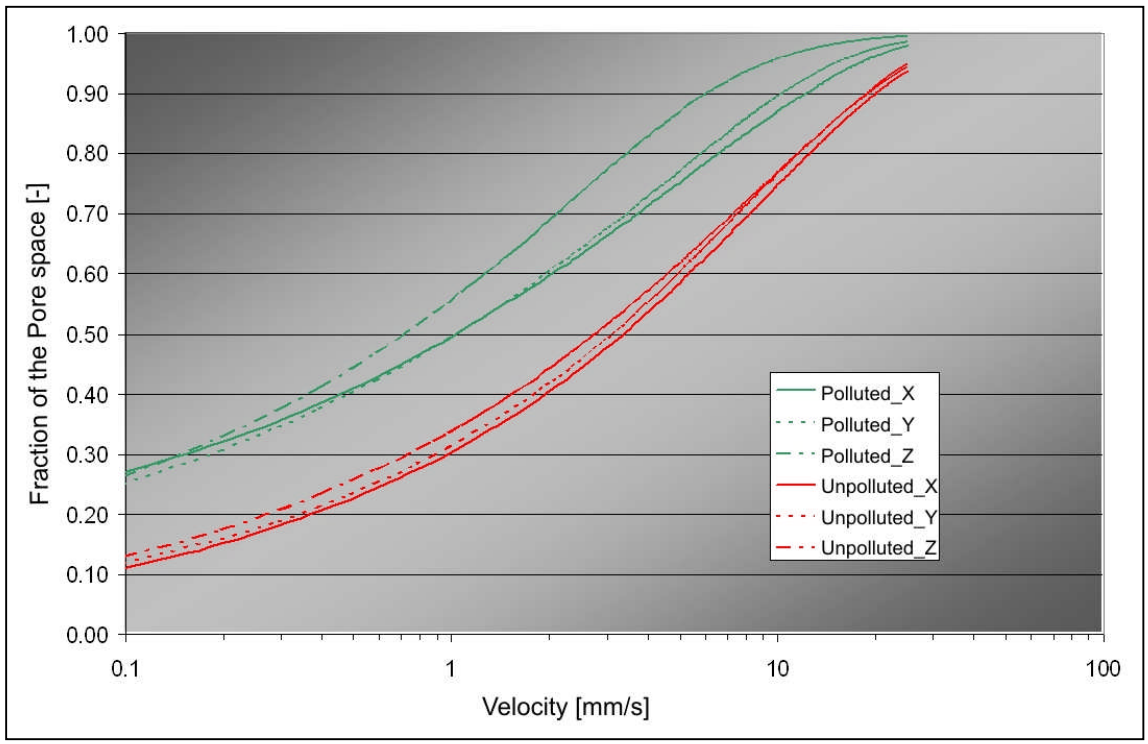

Figure 8: Distribution of velocities in the pores at different boundary conditions

During the next months, similar simulations will be done with a series of other OPA specimens, with polluted and unpolluted ones. The comparison of the different results will improve the understanding of pollution and particle transport mechanisms, and will convey an idea of the scattering of the simulations with the same OPA under the same boundary conditions

Another very important step in the evaluation of the results will be the consideration of the wall shear stresses inside the OPA. These stresses together with the velocity distribution allow a direct discussion of the pollution mechanisms of OPA.

3 CFD Simulation to the self-cleaning effects of OPA by traffic

As already mentioned, we wanted to investigate the self-cleaning effect of traffic with numerical tools during the research project. For this reason, we set up a simulation of a rolling tyre on a rain-wet pavement with a velocity of 80 km/h. The water film thickness was 3 mm. The numerical simulations were made with ANSYS CFX. The geometry of the simulation and the boundary conditions are shown in figure 9. The simulated air region had the dimensions 1.40 x 0.50 x 0.35 m. The air domain was connected at the bottom with an OPA domain of 1.40 x 0.50 x 0.05 m. The geometry of the warped tyre with grooves was calculated with a Finite Element tool by CONTINENTAL. The loads of the car were considered to be carried by the asphalt matrix without any influence on the fluid flow inside and outside of the OPA. The meshes for the simulations were generated with ICEM CFD. The resolution of the tetrahedron mesh was set to 0.5 mm near the tyre and about 2 cm near the lateral wall. The resulting meshes had about 6 million cells. The origin of the coordinate system was set in the axis of the tyre and, because of this, the asphalt layer had a velocity of -80 km/h. The momentum loss equation of the OPA

$$-\frac{\partial p}{\partial x_j} = \frac{\mu}{K} U_j + K_{loss} \rho \left|\mathrm{U}\right| U_j \tag{6}$$

had to be modified with a Galileo transformation. μ is the dynamic viscosity, K the permeability and K_{loss} an empiric loss coefficient. The tyre had a rotation velocity. At the inlet, the incoming air velocity was -80 km/h.

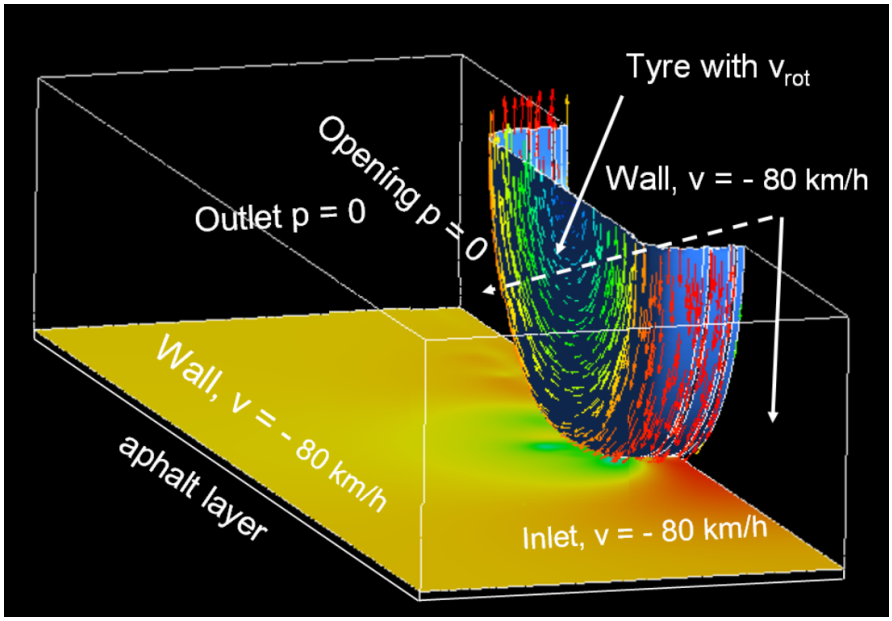

Figure 9: Boundary conditions of the CFD-Simulation. At the pavement surface the pressure is displayed. The stagnation pressure in front of the tyre and the low pressure zone at the lateral side due to the air acceleration can be easily observed.

The water level was set to 3 mm on top of the pavement. Below that level, only water enters the domains, above this level only air. At the top of the air region, an opening boundary condition was set to avoid reflections which could influence the flow field. The results of the simulation (fig. 11) were compared with the real circumstances for plausibility on the basis of photos (fig. 10). In the display of the water surface, a spray zone at the lag behind the tire (red region) can be identified. The tyre displaces the water film of the pavement. The lane behind the tyre (grey region) can be clearly seen. The observations of the simulation results and the photographs do agree well.

Figure 10: Photographs of cars on a rain-wet pavement

In the simulation, the resistance of OPA against flow was described with flow parameters, which were obtained in laboratory tests [2]. Displaying the water surface inside the OPA, one can see that the rolling tyre carries out the water outside the asphalt matrix down to a depth of about 3 cm. Due to the fast acceleration of the water inside the OPA, high fluid velocities were induced, which explain the self-cleaning effect of traffic.

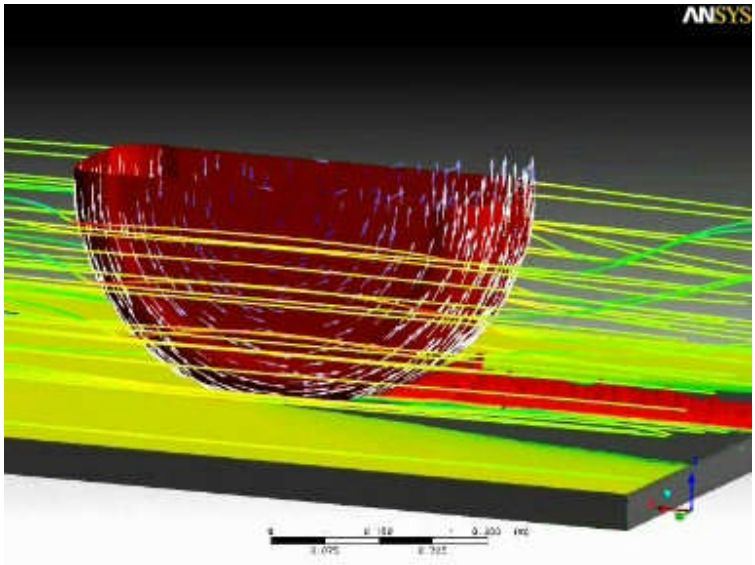

Figure 11: Simulation of a rolling type on rain-wet pavement with a velocity of 80 km/h. Streamlines and isosurface of the water surface

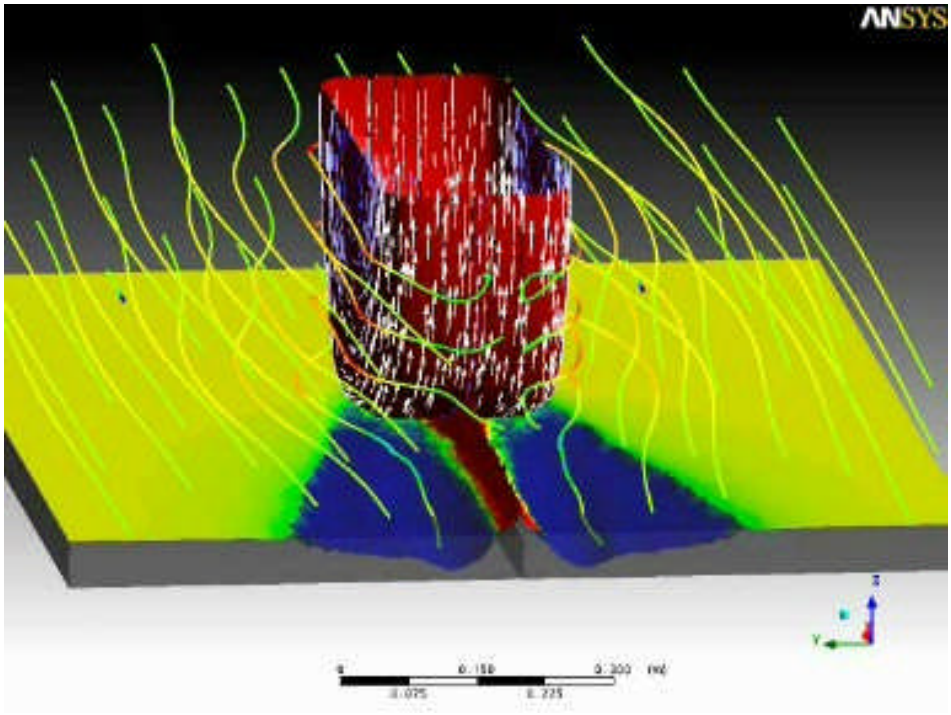

Figure 12: Water is carried out of the asphalt matrix by the rolling tyre, which explains the self-cleaning effect of traffic.

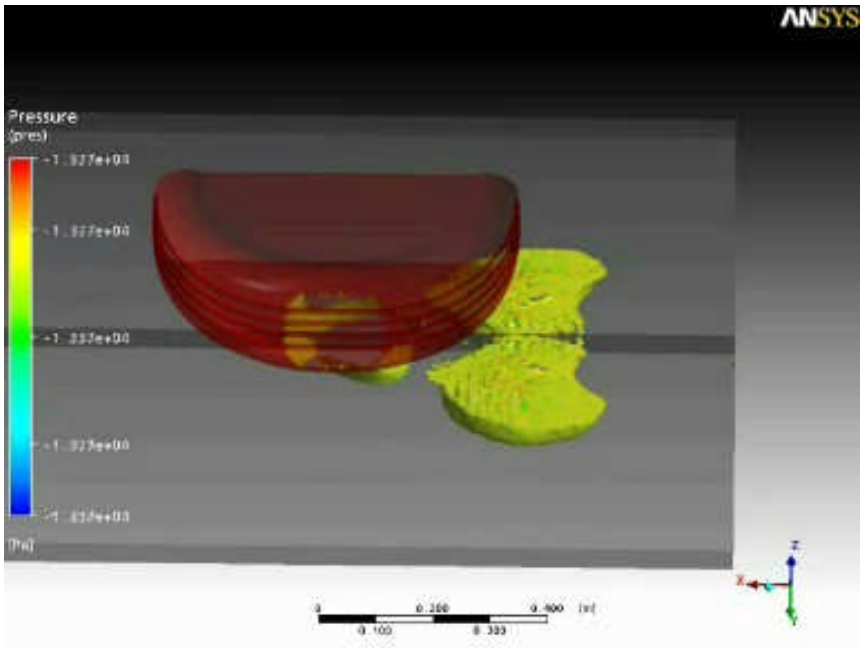

Figure 12: Isosurface of the low pressure zone of –13 kPa inside the OPA matrix.

Finally, the pressure field inside the OPA was analysed. Due to the rolling tyre with a velocity of 80 km/h a low pressure zone behind the tyre is generated with up to -0.2 bar (fig.12). The low pressure is the main reason for the acceleration of water towards the OPA surface and eventually the self-cleaning effect of OPA due to traffic.

5 Conclusions

In this paper numerical work is presented, which examines the detailed flow inside the pore structure of OPA. To acquire information about the anisotropy of the flow resistance and about the inhomogeneity of the flow in the OPA, detailed simulations of the pass-through of the resolved pores were done. Therefore, the Navier-Stokes equations were solved directly on a mesh which resolves the pore space. These simulations show a marked inhomogeneity of the velocity distribution in the pore space due to pollution. Moreover, the flow resistance differed at vertical and horizontal pass-through. In the next month a series of simulations will be done to allow a statistical discussion of the simulation results.

Finally the self-cleaning effect of traffic is examined. The simulation of a rolling type on a rain-wet pavement at a velocity of 80 km/h proofed the idea that the flow inside the OPA due to traffic can carry out water and pollution particles. Behind the type a low pressure zone can be identifies which is responsible for the high acceleration of water and air inside the asphalt matrix.

6 References

[1] Ferziger, J.H. and Peric, “Computational Methods for Fluid Dynamics”, Springer, 1997

[2] M. A. Haselbauer and M. Manhart, “Strömungsvorgänge in porösen Asphaltschichten”, In Fortschritte der Akustik, Tagungsband der DAGA, March 2007.

[3] N. Peller, A. Le Duc, F. Tremblay, and M. Manhart, “High-order stable interpolations for immersed boundary methods”, International Journal for Numerical Methods in Fluids 52 (3) (2006) 1174-1193.